COB-2019-0890
ANALYSIS OF EROSIVE DEMAGE IN FLAIL MOWER PROTECTIVE FRAME FLV 225

Otávio Almeida Gomes Pereira
University of Brazilian – UnB – Darcy Ribeiro University Campus, Brasília-DF | CEP 70910-900
otaviosae@gmail.com

Samuel Gustavo Alves Araújo
University of Brazilian – UnB – Darcy Ribeiro University Campus, Brasília-DF | CEP 70910-900
samuelgustavo95@hotmail.com

Thiago Doca
University of Brazilian – UnB – Darcy Ribeiro University Campus, Brasília-DF | CEP 70910-900
doca@unb.com

Abstract.
This work presents a failure analysis of the frame of the grass cutting system of a Flail Mower model FLV 225 (Herder). Studies on the impact and erosive wear are performed aiming to minimize the damage to this protective component. The speed of the particles is evaluated at both the collision stage and ejection stage. An erosive wear analysis is provided to quantify the volume of material lost due to the impact of the projectile against the frame. To minimize damage, surface treatments and protective coatings are investigated. The methodology is based on numerical modeling via the Abaqus commercial package. Two representative geometries for the impact particles are adopted. Different shapes, weights and impact angles are analyzed. It was demonstrated that the sharp particles are the most harmful to the frame.

Keywords: Impact, Erosive Wear, Numerical Modeling, Surface Enhancements

1. INTRODUCTION

The Federal District has millions of square meters of grassy areas. For the maintenance of these grassy areas the most common equipment used are the flail mowers. Motorized flail mower is a cutting equipment used in agricultural applications, gardening and maintenance of urban green areas. Tractor mowers are designed for applications that require high power and cutting capacity. There are basically four types of tractor mowers, as depicted in Fig. 1.

a) Reel Mower b) Rotary Mower c) Sickler Mower d) Flail Mower
Figure 1 – Type of Mower (TBN, 2015)

One of the main challenges for companies that use this equipment is reducing the cost of maintenance. This high cost is due to the lack of adequate maintenance planning for each machine. The Figure 2 depicts the equipment studied.

Figure 2 – Flail Mower FLV 225.

The goal of this work is to analyze the frame of the flail mower type model FLV 225. The analysis will be divided into two topics: i) impact and ii) erosive wear. Description of the problem is presented in Section 2. The impact analysis consists in quantifying the velocity that the particles hit the frame which leads to identification of the type of impact. The evaluation of the erosive wear phenomena will indicate the number of impact cycles that the frame can endure. Computational simulations are performed using with Abaqus CAE v6.14® commercial package. Protective solutions area proposed in section.

1.1 PROCESS OF CARCASS FAILURE

The process of carcass failure is caused by the impact of particles with varied geometries and masses. This phenomenon happens due to the rotation of the central axis, which by means of an angular movement, the blades that are connected, impact on the projectile and then it is thrown against the carcass. Figure 3 represents the failure process and Figure 4 is a real damage of the carcass due to particle impact.
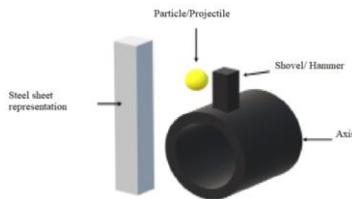

Figure 3 – Representation of the fault process.

Figure 4 – Real damage in carcass.

1.2 EROSIVE WEAR

Erosive wear has been studied for several decades, due to its great technological importance. It is a type of degradation of materials that covers many industries, such as aeronautics, transportation and others. Erosion is a process of abrasive wear so that the repeated impact of small particles moving the fluid against a surface results in the removal of the material from that surface. (HUTCHINGS,1974). According to Bittar (1963) erosion is defined as material damage caused by the attack of entrained particles in a fluid system, impacting the surface at high speed.

Some of the variables that affect erosion can be classified as three Topics (FINNIE, 1971):

1. Impact variables describing the flow of particles
    a) Angle of impact;
    b) Velocity of particle;
    c) Concentration of particles;
    d) Rotation of particles on impact;
    e) Time of impact.
2. Variables of particles
    a) Form of the particle;
    b) Density of the particle;
    c) Size of the particle.
3. Variables of material
    a) Modulus of Young;
    b) Coefficient of Poisson;
    c) Plastic behavior;
    d) Nature of the entrainment fluid and its temperature;
    e) Fault behavior;
    f) Hardness of materials.

1.3 IMPACTOLOGY

The part of the mechanics that aims to study the nature of impact is called impactology. Its fundamental goal is to evaluate the forces that are released at the time of mechanical shock. It can be divided into two parts, which are: (BERTOLDO,2013)

1) Inertial Impact: Studies the shock of a moving particle against a fixed target at rest.
2) Kinematic Impact: Studies the mechanical shock between moving bodies.

This study will be limited to inertial impact analysis, where it will be considered the evaluation of the impact force of a body, in uniformly varied motion, when it crashes against a resting steel plate.

2. MATERIAL AND METHODS

The work was divided into two topics with some subtopics. The first topic is about the preliminary study that includes:

• Three-Dimensional modeling

The brushcutter is a farm equipment composed of several parts for full operation, within each main part there are several components. The modeled central area is called the shredding unit and has greater damage due to particle impacts. This equipment shown in figure 5 has a cutting width of 2.25 m, with a rotation of 2100 rpm weighing about 590 kg.

Figure 5 - Modeling of the rendered bulkhead.

• Hardness test

The Brinell hardness value of the protection structure is 131.1 HBW5/350. The Table 1 shows the results of the hardness tests. From this, when checking in the catalogs of the steel manufacturers (Gerdau and Arcelor Mittal) it was found that the steel that matches the hardness results is SAE 1020 steel.

Table 1 - Results of the Brinell hardness test.

Test	Brinell hardness test	
	Hardness value	
1	133.2	HBW5/250
2	130.5	HBW5/250
3	130.4	HBW5/250
4	130.3	HBW5/250
Average	**131.1 HBW5/250**	
Standard Deviation	**1.4**	

• Calculation of particle velocity

To perform the calculation of the velocity of the particle impacting the bulkhead requires some equipment variables, such as: angular speed and radius of the axis of rotation and the size of the hammer. The rotation of the Herder FLV 225 mower from the Herder catalog is 2100 rpm, the rotor shaft has a diameter of 160 mm or 0.16 m and the hammer has a length of 100 mm or 0.10 m which was measured on place, using a measuring tape and a caliper. Initially it is converted from rpm to rad / s with equation (1).

$$\omega = \frac{rad}{s} = \frac{rpm * 2 * n}{60} \tag{1}$$

$$v = \omega * r \tag{2}$$

From equation (1), a conversion from 2100 rpm to 70 π rad / s was obtained. Applying this result and the radius of the rotor axis in equation (2), we will find that the velocity of the particle impacting the bulkhead is 39.58 m / s.

• Properties of target material

From the hardness test, it was found that the material used in the bulkhead is SAE 1020 Steel. The properties of the material used in the analysis are listed in Tables 2 and 3. To obtain a modeling pertinent to the behavior of the material, the formulation of Johnson and Cook was used.

Table 2: Properties of AISI 1020 steel (MEDYANIK, 2007)

Material	Density [kg/m³]	Modulus of elasticity [GPa]	Poisson coefficient	β	Specific heat [J/kg.K]
Steel	7830	200	0.3	0.9	477

Table 3: Parameters of the plasticity model (JASPER, 2002)

A	B	n	m	T_m	T_r	c	$\dot{\varepsilon}$
333	737	0.15	1.46	1793	298	0.008	1

The criterion of damage used was the initiation criterion and damage evolution law for ductile materials. The damage parameters are in Table 4.

Table 4: Johnson and Cook Damage Criteria Parameters. (JOHNSON AND COOK, 1985)

Material	d_1	d_2	d_3	d_4	d_5	$T_m[k]$	$T_r[K]$	$\dot{\varepsilon}[s^{-1}]$
Steel	0.05	3.44	2.12	0.002	0.61	1793	298	1

• Properties of the projectile

The material of the projectiles is not defined as being considered a rigid body (undeformable), therefore there is no need to specify which type of material is used, this is because this solid does not deform, nor the stresses are computed. However, the mass of the projectile must be specified. In order to approach reality with the projectiles that impact on the shield, the weight of each projectile was used as 500 g. This property is applied at the reference point (RP). For the spherical particles, half of the total mass value was associated with the symmetry boundary condition.

The second topic is addressed to modeling number, which encompasses the following subtopics:

• Type of contact

Knowing that the coefficient of friction is a dimensionless number that depends on the roughness of the face of the body that is supported and the surface of contact and that the rougher the body or the surface the greater the coefficient, the coefficient was considered equal to 0.2 (ELTOGBY, 2005). The contact used is surface-to-surface (Explicit) where the outer surfaces of the rigid geometries are the "master" surfaces and the nodes of the geometry related to the target material being the "slave" surfaces.

• Simulation of surface erosion

In order to model the morphology of the surface eroded by the particle impacts, two models were considered. In the first model, the erodent particle is spherical in shape and the second is a sharp object. The simulations were based on an assembly containing a deformable rectangular plate 100 x 6.35 x 100 mm for the target material and the three rigid particles of the same geometry in each analysis as erodent particles oriented at 90 ° and 30 ° with the surface of the plate, aligned and spaced apart.

• Geometries

In the simulation with rigid spherical particles, a sphere of diameter of 50 mm were used, as see in Figure 6a. In the simulation with pointed particles, a solid with 31 mm of height, 50 mm of thickness, 10 mm of length and an angulation at the tip of the solid of 30 ° was used (Figure 6b).

The target material used will be the same for both types of simulation, a deformable plate with dimensions of 100 x 6.35 x 100 mm, as depicted in Figure 6c.
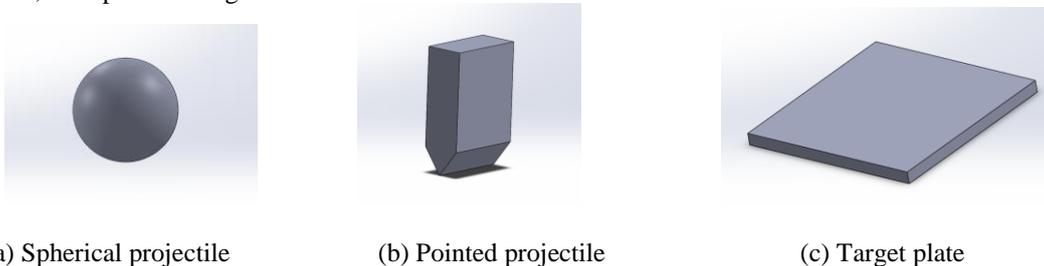

(a) Spherical projectile   (b) Pointed projectile   (c) Target plate

Figure 6 - Types of solids used in the simulation.

• Contour conditions

In the erodent (spherical and pointed) particles were restricted the lateral displacement of the same and the rotation in the three directions. The base of the target plate was created between the ends of the plate and the vertical displacement of the plate was restricted.

• **Velocity**

In the "predefined field" command of the software, a velocity of 39.58 m/s, with an impact angle of 90° and 30° (between the velocity vector and the surface) was associated with each erodent particle, in its respective analysis flat on the plate).

• **Mesh used**

A mesh sensitivity analysis was performed on the size of the elements and type of integration. Considering the computational cost and stress distributions obtained, first solid elements and reduced integration were adopted for geometries of the target material. The elements of the geometry related to the target material are C3D8R type: 3D stress family, linear order, 8-node hexahedron, with reduced integration, first order and with maximum degradation (element is eliminated from the analysis when the overall damage is maximum, equal to 1). For the target material, the most refined mesh in the central impact region was considered, maintaining element control by adopting 40 elements. For the projectile, it was considered 20 elements, however, the whole projectile was in the same mesh, without distinction of meshes in the same material.

• **Variables analyzed**

To analyze erosive wear, it is necessary to consider some variables that affect wear. Therefore, in this work the influence of the impact angle, the projectile mass and the geometry will be analyzed. Some variables were not altered because they are fixed in this type of situation, for example, the velocity of the projectile, which impacts on the bulkhead and the hardness of the target material.

In order to obtain more significant results, the impact of spherical and pointed particles, in different angles was evaluated, impacting on the target material with the same properties of the target material. As can be seen in the figures 5 and figures 6.
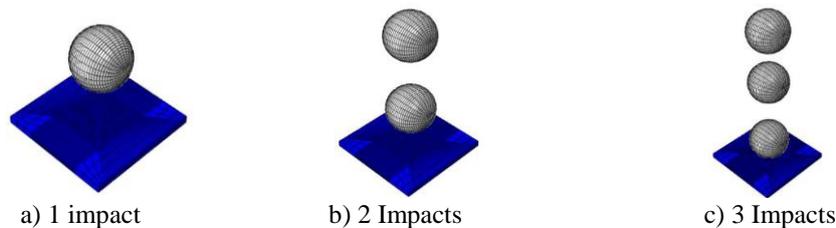

a) 1 impact   b) 2 Impacts   c) 3 Impacts

Figure 8 – Initial assembly for 90° simulation.

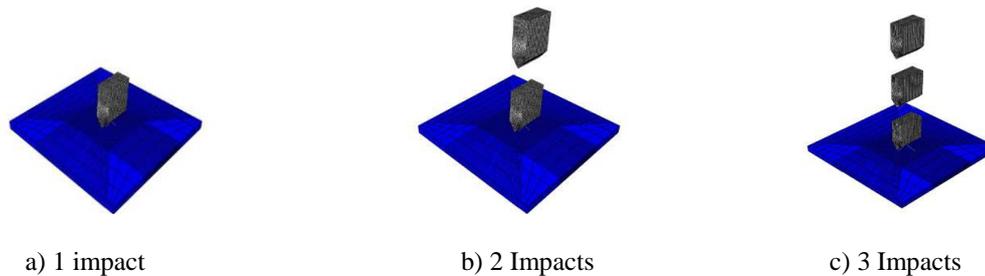a) 1 impact   b) 2 Impacts   c) 3 Impacts

Figure 9 – Initial assembly for simulation of sharp objects at 90°.

3. RESULTS AND DISCUSSIONS

This section presents the results for the impact of the spherical particles, sharp particles and the simulation of the protective structure.

3.1 SPHERICAL PARTICLE IMPACTS

An impact simulation was performed on a 1020 steel plate with dimensions 100 x 100 x 6.35 mm and 3 spherical particles, each weighing 500 grams, at a 90 ° angle, which collided sequentially in the same place, in order to analyze a condition critical. The stress distribution for each impact is shown in Figure 10. It is noted that successive impacts of spherical particles generate a progressive increase of the stresses. Having an increase in the deformation of the bulkhead caused by each impact.
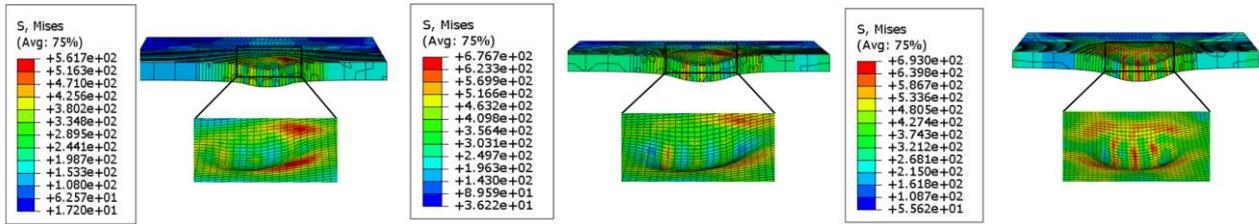
a) Distribution of stress of the 1st impact.   b) Distribution of stress of the 2 st impact.   c) Distribution of stress of the 3 st impact.

Figure 10 - Equivalent stresses (S- von Mises) [Mpa].

The value of von Mises obtained in the simulation in the critical region for the first impact was 561 MPa, for the second impact it was 676 MPa and for the third impact it was 693 MPa. It is also worth noting that in this type of ball - plate (flat) impact simulation, the erosion process is smaller, with a predominance of plastic deformation.

Figure 12 shows the distribution of equivalent plastic deformation (PEEQ - scalar that presents the resulting plastic deformations in the 3 directions) after each particle impacting the bulkhead. It is possible to verify the progressive increase of PEEQ. The values obtained were 0.145 for the first impact, 0.180 for the second impact and 0.216 for the third impact.
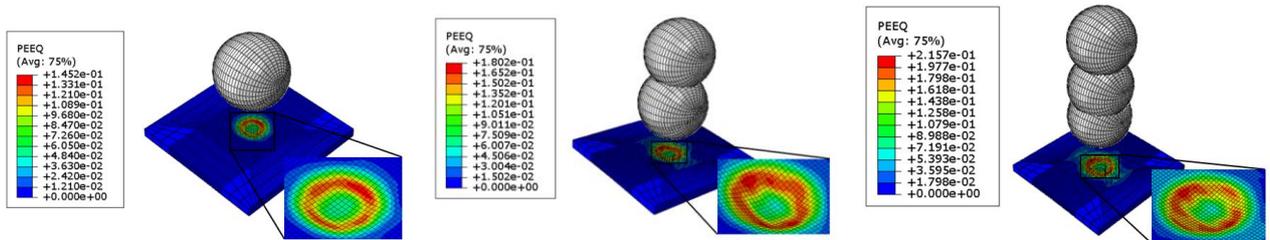
a) PEEQ - 1st impact.   b) PEEQ - 2st impact.   c) PEEQ - 3st impact.

Figure 12 - Equivalent plastic deformation (PEEQ) for an angle of 90 °.

Analyzing the results of equivalent plastic deformation and considering a linearity of these results, it is possible to estimate that every 15 impacts of a body with spherical geometry in the same place and similar mass will have a PEEQ of 1. Therefore, approximately 96 impacts would produce a PEEQ of ± 6.4, breaking the bulkhead.

Finally, it is verified that the simulation with spherical particles at 90 °, presented satisfactory results, demonstrating that for this geometry, plastic deformation damages are more common and that the results of deformations are compatible with the material of the bulkhead.

Subsequently, the effect of the inclined impact was verified at an angle of 30 ° in order to measure the influence of geometry and slope on erosive wear. In the critical region the von Mises stress in the first impact was 691 MPa, in the second impact it was 775 MPa and in the third impact was 843 MPa, data presented in Figure 13. Comparing the equivalent stress between the 90 ° and 30 ° simulation, it is possible to verify that in the case of inclined impact there was a significant increase of the stress in the contact region of approximately 20%. This confirms that the impact inclined at 30 ° is more critical than at 90 °.
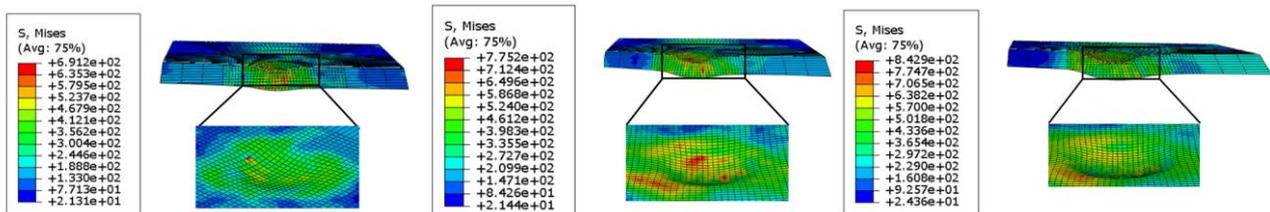
a) Distribution of stress of the 1st impact.   b) Distribution of stress of the 2 st impact.   c) Distribution of stress of the 3 st impact.

Figure 13 - Equivalent stresses (S- von Mises) [MPa].

When evaluating the equivalent plastic deformation (PEEQ) of the 30 ° simulation, we observed that the results remained close to the 90 ° simulation. The Figure 14 shows that at 90 ° the critical stress is distributed throughout the contact area, and in the case of impact at 30 ° the critical stress is concentrated in the middle of the contact area, causing it to have a higher equivalent stress. However, it maintains the value of the resulting plastic deformation in all directions

(PEEQ). In this type of geometry, the erosive wear is lower even by varying the angle, predominating the plastic deformation.
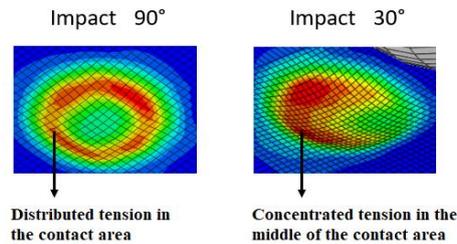

Figure 14 - Comparison of stress varying the angle.

3.2 IMPACTS IMPACT OF SHARP PARTICLES

An impact simulation was performed on a 1020 steel plate with dimensions 100 x 100 x 6.35 mm and 3 sharp particles, each weighing 500 grams, at an angle of 90°, which collide sequentially in the same place, with the purpose of analyzing a critical condition. Figure 15 shows the three types of impact performed, and the layout of the objects to perform the simulation.
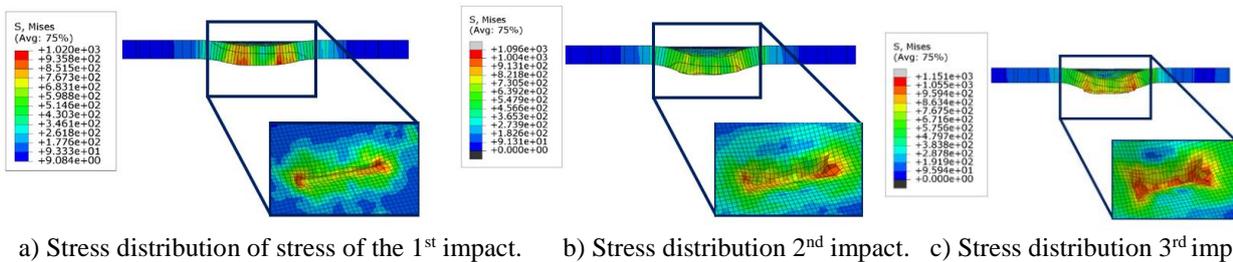

a) Stress distribution of stress of the 1st impact.   b) Stress distribution 2nd impact.   c) Stress distribution 3rd impact.

Figure 15 – Equivalent stress distributions (S- von Mises) [MPa].

From the impact simulations, it is possible to obtain the Von Misses stress in the critical region. For the first impact the highest stress was 1020 MPa, while the second impact was 1096 MPa and the third and higher stress was 1151 MPa.

Figure 16 shows the equivalent strains distribution (PEEQ- Scalar that presents the resulting plastic deformation in the 3 directions), it is noted that after each impact of the pointed object on the bulkhead, the PEEQ progressively increases until a certain impact. It is possible to analyze the values obtained from each impact, where the first is 0.4703 and second is 1.4380. The third impact, in which the theory is about the impact that will have the greatest accumulation of plastic deformation, has a lower value than the second impact. This value is due to the increase of the rigidity of the material by plastic deformation, in that it goes through a phenomenon that modifies the crystalline structure of the metal, known as hardening consequently modifies the mechanical properties of the material. When the material courses by changing the shape of its grain, it increases the amount of dislocations making it "harder" to deform, thereby increasing its mechanical strength, but the area of the impact section is decreasing due to a stretching of material, consequently reduces the body's ability to withstand loads.
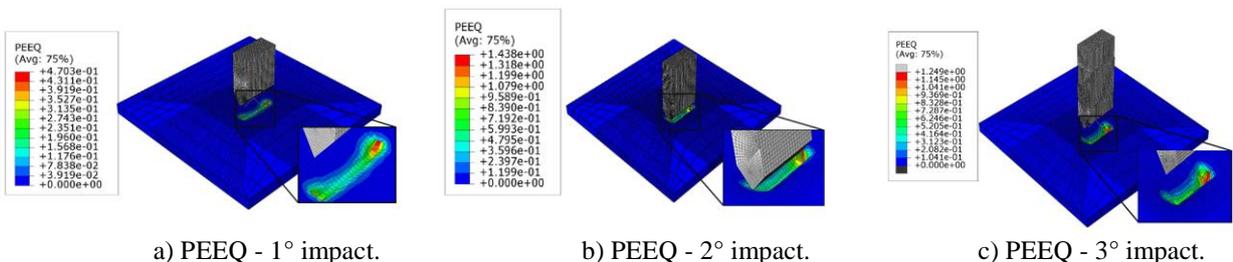
a) PEEQ - 1° impact.   b) PEEQ - 2° impact.   c) PEEQ - 3° impact.

Figure 16– Equivalent plastic deformation (PEEQ) for a 90 ° impact angle.

Analyzing the results of equivalent plastic deformation (PEEQ) and considering that there is no linearity of these results when it comes to a certain sharp particle impact, it is possible to estimate that in the next impact of a pointed body in the same place, with the same speed, the target material will fail because, because of the hardening of the material, its capacity to absorb loads will be less. Figure 17 shows a screen of a brush cutter that probably had the

impact of sharp objects, and after successive impacts the material crumbled, becoming a fragile material, and after other impacts the equipment failed and caused a hole in the bulkhead.
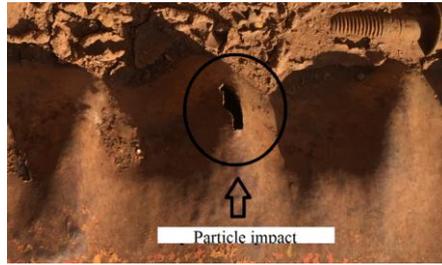

Figure 17 - Particle impact deformed bulkhead

Finally, to analyze erosive wear in this impact study, we compared the simulation with spherical particles and with pointed particles. It is possible to conclude that geometry is a factor that influences erosive wear and that the two geometries studied cause a progressive wear of the target material, however, the increase of this type of wear depends on the angle of inclination between the plate and the particle. Noting that erosive wear was relevant in the pointed particles, and that for a 90 ° angle this wear was lower than for an angle of 30 °, as we can see in Table 5.

Table 5: Equivalent plastic deformation (PEEQ) for angulation of 30 ° and 90 °.

	Spherical projectile		Pointed projectile	
	Impact 90°	Impact 30°	Impact 90°	Impact 30°
1° Impact	0.1452	0.137	0.4703	0.8277
2° Impact	0.1802	0.1821	1.438	1.141
3° Impact	0.2157	0.226	1.249	1.613

3.3 SIMULATIONS OF PROTECTION STRUCTURE FLV 225

A FLV 225 bulkhead simulation (modeled in SOLIDWORKS with real dimensions) was performed using the finite element package (ABAQUS). Several impacts of spherical and pointed geometry particles were reproduced in order to analyze the influence of the mass in causing damage to the bulkhead. Figure 6 shows the simulation assembly.
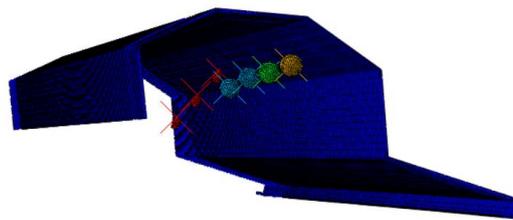

Figure 6 – Simulation of the FLV 225 trimmer screen.

The impacts were directed to the critical area of the bulkhead, having an angle of 47.5 ° between the particle and the impact site in the bulkhead (real case). The speed used was 39.58 m/s.

Figure 7 shows the stress results after the impact of each particle. Analyzing the results, we can verify that for spherical geometry, particles with masses less than 250 grams do not cause damage to the structure (seen in particle 4) and for pointed geometries, particles with mass less than 200 grams do not cause damage to the structure particle 7) because they were below the allowable stress. It is important to note that pointed particles are more critical than spherical particles, as evidenced in this simulation. For a spherical particle to cause damage to the bulkhead, it must have a mass greater than 250 grams, in the case of a pointed particle, only having 200 grams to cause damage to the bulkhead.
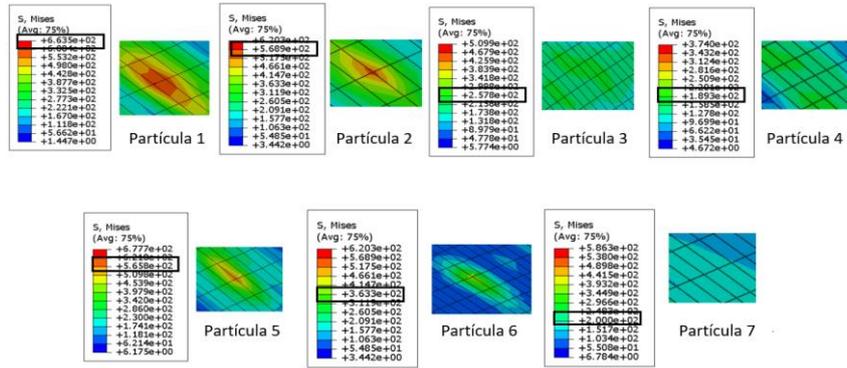
Figure 7 – Stress output of the bulkhead simulation.

It was also evaluated the PEEQ, validating that particles with mass less than 200 grams for pointed geometries and particles with mass less than 250 grams for spherical geometries do not cause damages to the bulkhead. The total results are shown in Figure 8 shows the damage that each particle caused, noting that in particle 4 and 7 there was no considered damage to the shield.
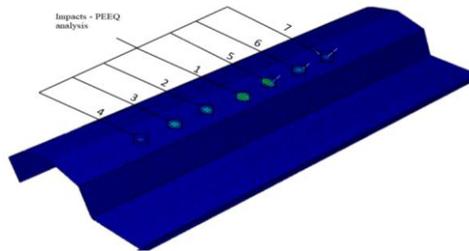

Figure 8 – Damage of each impact.

Subsequently with the objective of simulating dozens of impacts on the bulkhead, in which case it happens in an operation of the equipment when mowing the grass, a numerical simulation was made using 100 impacts with spherical geometry of 500 grams and pointed of 400 grams. It is a critical situation, because in reality hundreds of impacts happen, but of particles with different geometry and mass varied, thus not all particles cause damage to the bulkhead. Figure 9 shows the simulation assembly.
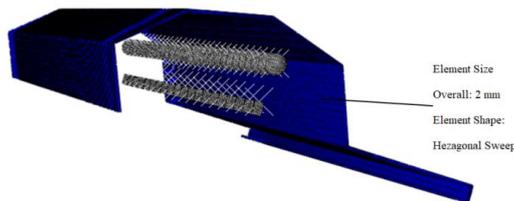

Figure 9 – Simulation assembly.

The objective of this simulation is to compare the critical area between the simulation and reality, highlighting the damage caused by these particles, as shown in Figure 10.

a) Critical region of the bulkhead in the simulation.   b) Critical region of the bulkhead in reality.

Figure 10 – Critical region.

4. CONCLUSIONS

A study of the degradation of the bulkhead over time due to the impact of particles is presented. Hardness test was performed to verify the material used in the bulkheads, which determined that SAE 1020 steel was employed.

A three-dimensional model of the bulkhead was produced using the SolidWorks software. This model was simulated using the finite element package Abaqus CAE 6.14. It was possible to notice, from inspections in the brush cutters, that the impact of particles was the cause of the erosive wear and the plastic deformations over the surface. However, the damage observed near the fixation area should also be analyzed in detail as they might start a fatigue process in that region. During the machine inspection, a measure the diameter of the axis of rotation was performed and with the angular velocity of the axis it was possible to find the terminal speed of the particle when it hits the frame.

Numerical models of two particles were produced to assess the erosive effects of the impacts. Analysis with the spherical projectile, has shown severe plastic deformation and as the number of impacts increase a higher level of stress is induced. However, when the angulation is changed, from 90º to 30º the difference of equivalent plastic deformation (PEEQ) is small to the point of being negligible. Moreover, the projectile with a 90º impact causes a large plastic deformation, such that in the third impact its observed the hardening of the material.

Performing the simulation with the surface coating does not It was possible due to the need to perform the Charpy test and the tensile test to acquire the material properties and the Johnson and Cook constants. Therefore, it is suggested as future work to perform these tests applying the coating on a specimen to lift the constants of Johnson and Cook. After obtaining these data from the experimental test, it is suggested to perform the computer simulation with the adopted surface coating.

5. REFERENCES

BERTOLDO, L. Dinâmica do impulso e do impacto, 2013.

ELTOBGY, M. S., E. Ng, ELBESTAWI, M. A. Finite element modeling of erosive wear. International Journal of Machine Tools & Manufacture 45 (2005) 1337-1346.

I.M. HUTCHINGS, Particle erosion of ductile metals: a mechanism of material removal, Wear 27 (1974)

I. FINNIE, Some observations on erosion of ductile metals, Wear,1971.

Jaspers, S. P. F. C., & Dautzenberg, J. H. (2002). Material Behavior in Conditions Similar to Metal Cutting: Flow Stress in the Primary Shear Zone. J. Mater. Process. Technol., Vol. 122, pp. 322–330.

J. BITTER, A study of erosion phenomena, part 1, Wear 6 ,1963.

JOHNSON, G. R., COOK, W.H. – Fracture characteristics of three metals subjected to various strain rates, temperatures and pressures – Engineering Fracture Mechanics, vol 21, No. 1, 1985, pages 31-48.

MEDYANIK, S. N.; LIU, W. K.; LI, S. On criteria for dynamic adiabatic shear band propagation. Journal of the Mechanics and Physics of Solids 55 (2007)

TBN. What is the Right Mower Type for Your Situation?. 2015. Online; Acessado em: 25-03-2018. Disponível em: < http://www.tractorbynet.com/lawn-garden/mowing/what-is-the-right-mower-type-for-your-situation/>.

6. RESPONSIBILITY NOTICE

The authors are only responsible for the printed material included in this paper.